PHYSICAL REVIEW B, VOLUME 65, 094415

# Possible impurity-induced ferromagnetism in II-Ge-$V_2$ chalcopyrite semiconductors

Yu-Jun Zhao
*Department of Physics & Astronomy, Northwestern University, Evanston, Illinois 60208*

S. Picozzi and A. Continenza
*Istituto Nazionale di Fisica della Materia (INFM), Dipartimento di Fisica, Univ. degli Studi di L'Aquila, I-67010 Coppito, L'Aquila, Italy*

W. T. Geng* and A. J. Freeman
*Department of Physics & Astronomy, Northwestern University, Evanston, Illinois 60208*

(Received 24 September 2001; published 11 February 2002)

Recently reported room-temperature ferromagnetic (FM) semiconductors $Cd_{1-x}Mn_xGeP_2$ and $Zn_{1-x}Mn_xGeP_2$ point to a possible important role of II-IV-$V_2$ chalcopyrite semiconductors in "spintronic" studies. Here, structural, electronic, and magnetic properties of (i) Mn-doped II-Ge-$VI_2$ (II=Zn or Cd and V=P or As) chalcopyrites and (ii) the role of S as impurity in $Cd_{1-x}Mn_xGeP_2$ are studied by first-principles density functional calculations. We find that the total energy of the antiferromagnetic (AFM) state is lower than the corresponding FM state for all systems with Mn composition $x=0.25$, 0.50, and 1.0. This prediction is in agreement with a recent experimental finding that $Zn_{1-x}Mn_xGeP_2$ experiences a FM to AFM transition for $T$ less than 47 K. Furthermore, a possible transition to the half-metallic FM phase is predicted in $Cd_{1-x}Mn_xGeP_2$ due to the electrons introduced by *n*-type S doping, which indicates the importance of carriers for FM coupling in magnetic semiconductors. As expected, the total magnetic moment for the FM phase is reduced by one $\mu_B$ with each S substituting P.

DOI: 10.1103/PhysRevB.65.094415 PACS number(s): 75.50.Pp, 75.30.Hx

## I. INTRODUCTION

Magnetoelectronics ("spintronics") is a new discipline which has recently become one of the key research areas connecting the semiconductor industry (from the charge degree of freedom) and magnetic recording (from the spin degree of freedom).[1] For example, the recent demonstration of the electric-field control of ferromagnetism (FM) in a thin-film semiconducting alloy is expected to have a great technological impact.[1] While these developments hold considerable promise, in principle, the limiting factor that represents a serious bottleneck for their practical spintronic applications is the fact that both the observed ferromagnetism and the attractive injection phenomena are essentially limited to low temperature in Mn-doped GaAs semiconductors. This bottleneck clearly arises from the specific properties of the magnetic semiconductor materials that are currently available, which until recently have been limited primarily to III-V-based alloys containing Mn ions.[2]

The chalcopyrite differs from the zinc-blende crystal structure by a doubling of the unit cell along a fourfold axis, rendering the system body-centered tetragonal. The II-IV-$V_2$ chalcopyrites are easily seen to be an extension of the III-V zinc-blende compounds, the combination II-IV playing the role of two group-III atoms and jointly supplying three valence electrons per atom, to combine with the five electrons provided by each group-V ion. The expected special advantage of these systems is that Mn can be substituted readily for II cations, as demonstrated[3] for $II_{1-x}Mn_xIV$ alloys with $x$ up to 1.0 without the formation of structural defects, owing to the natural tendency of Mn to adopt a $+2$ state. Medvedkin *et al.*[4] incorporated high Mn concentrations into the surface region of a II-IV-$V_2$-type chalcopyrite semiconductor $CdGeP_2$ by vacuum deposition of Mn on a single-crystal surface followed by a solid-phase reaction at elevated temperatures. An important finding reported by Medvedkin *et al.* is room-temperature ferromagnetism in highly doped $Cd_{1-x}Mn_xGeP_2$—which constitutes a tremendous improvement from the $T_C$ of 110 K found in $Ga_{1-x}Mn_xAs$ for $x=0.053$. Our previous work[5] studied the $Cd_{1-x}Mn_xGeP_2$ system by first-principles theoretical calculations, employing both the full-potential linearized augmented-plane-wave[6] (FLAPW) and $DMol^3$ methods[7] within both the local density approximation (LDA) and the generalized gradient approximation (GGA). We found that the total energy of the antiferromagnetic (AFM) state is lower than the corresponding FM state for $Cd_{1-x}Mn_xGeP_2$ for $x=0.25$, 0.50, and 1.0.

Very recently, Cho *et al.*[8] found another room-temperature FM semiconductor in II-Ge-$V_2$ chalcopyrite $Zn_{1-x}Mn_xGeP_2$ with $T_C=312$ K. In addition, they reported that the AFM state exists for $Zn_{1-x}Mn_xGeP_2$ at temperatures below 47 K, which is consistent with the previous experimental and theoretical results in $Cd_{1-x}Mn_xGeP_2$. This confirms the possible more important role of II-Ge-$V_2$ chalcopyrites in "spintronic" applications and so calls for more theoretical and experimental studies of this class of materials.

In this paper, we report results of a systematic investigation of the electronic and magnetic properties of $Zn_{1-x}Mn_xGeP_2$, $Zn_{1-x}Mn_xGeAs_2$, $Cd_{1-x}Mn_xGeP_2$, and $Cd_{1-x}Mn_xGeAs_2$ with both the FLAPW and $DMol^3$ methods. In Sec. II, we report some computational technicalities; the lattice constant of these systems are discussed in Sec. III; we focus on electronic and magnetic structures of these systems in Sec. IV; in Sec. V, the possible transition to a FM state by S impurity doping is discussed.

 ©2002 The American Physical Society

## II. METHODOLOGY

We employ two first-principles electronic structure methods to determine the structural, electronic, and magnetic properties. DMol$^3$ (i.e., density functional theory for molecules and three-dimensional periodic solids[7]) uses fast convergent three-dimensional numerical integrations to calculate the matrix elements occurring in the Ritz variational method.[9] It calculates variational self-consistent solutions to the density functional theory (DFT) equations, expressed in a numerical atomic orbital basis.[9,7] The DMol$^3$ method has been successfully applied to the complex structure of the $BaTiO_3$ grain boundary[10] and a spin-polarized chalcopyrite magnetic semiconductor,[5] and proved to be a powerful tool for structural optimization. The DMol$^3$ method, while not as precise as the FLAPW method, is appropriate to give a reasonable description of the internal structure and electronic properties considering the reduced computational effort. In this work, a double set of numerical valence functions with the local basis cutoff $R_c$ of 9.0 a.u. is employed. The relativistic treatments for the atoms are done via a pseudopotential[11] acting on all electrons to get scalar relativistic corrections for the relevant valence orbitals. We employ the GGA functional of Perdew, Burke, and Ernzerhof[12] (PBE), which has been used successfully in studies of other magnetic semiconductors.[5,13,14] DMol$^3$ is used to optimize the internal degrees of freedom of all these $II_{1-x}Mn_xGeV_2$ systems and the final results are checked by the highly precise FLAPW method.[6]

In the FLAPW method, no shape approximations are made for the wave functions, charge density, and potential. For all atoms, the core states are treated fully relativistically and the valence states are treated semirelativistically (i.e., without spin-orbit coupling). Muffin-tin (MT) radii for Cd, Zn, Ge, and Mn are chosen to be 2.30 a.u., while 1.8 a.u. for P and S and 2.0 a.u. for As are used, respectively. An energy cutoff of 9.0 Ry is employed for the augmented-plane-wave basis to describe the wave functions in the interstitial region, and a 49 Ry cutoff is used for the star functions depicting the charge density and potential. Within the MT spheres, lattice harmonics with angular momentum $l$ up to 8 are adopted. The GGA functional with the same formula as in DMol$^3$ [i.e., PBE (Ref. 12)] is employed with the corresponding DMol$^3$ optimized structure. The calculated forces are found to be well balanced in the FLAPW calculation, which indicates that the DMol$^3$ optimization is quite consistent with the FLAPW calculation for all these $II_{1-x}Mn_xGeV_2$ systems.

## III. STRUCTURAL PROPERTIES

One problem in studying the electronic structure of a doped system is posed by the changes of the crystal structure on doping. Our previous works[5,14,15] show that the GGA gives a better lattice constant for Mn-related systems, such as MnAs and $MnGeP_2$, but that it overestimates some pure $s$-$p$ semiconductors, such as GaAs and $CdGeP_2$. Fortunately, Jaffe and Zunger proposed some effective rules for the lattice constant in $ABC_2$ chalcopyrite structures.[16] The nearest-neighbor anion-cation bond lengths are given by

$$R_{AC}=[u^2+(1+\eta^2)/16]^{1/2}a, \tag{1}$$

$$R_{BC}=\left[\left(u-\frac{1}{2}\right)^2+(1+\eta^2)/16\right]^{1/2}a, \tag{2}$$

where $\eta\equiv c/2a$. An enormous body of crystallographic studies has been directed at defining elemental radii that add up to the measured bond length $R_{ij}\simeq r_i+r_j$, which is referred to as the "conservation of tetrahedral bonds" (CTB).[16] The implication of this principle for the structural parameters $a$, $\eta$, and $u$ of $ABC_2$ compounds is that these degrees of freedom would attain values that minimize simultaneously the difference between the actual anion-cation bond lengths $R_{AC}$ and $R_{BC}$ and the sums of the elemental radii.[16]

Although $R_{AC}$ and $R_{BC}$ could be obtained from the elemental radii and the CTB rule, the $a$, $u$, and $\eta$ could not be obtained quantitatively unless another restriction is applied. Abrahams and Bernstein[17] proposed that the bond angles at the $B$ atom in $ABC_2$ chalcopyrites would have the ideal tetrahedral values, which leads to

$$a^2=\frac{12\alpha^2}{2\beta+\alpha-[(2\beta+\alpha)^2-18\alpha^2]^{1/2}}, \tag{3}$$

$$\eta^2=\frac{8(\beta-\alpha)}{3\alpha^2}, \tag{4}$$

where $\alpha=R_{AC}^2-R_{BC}^2$ and $\beta=R_{AC}^2+R_{BC}^2$.

As noted by Abrahams and Bernstein,[17] this model gives good agreement for the II-IV-$V_2$ compounds when the column-IV atom is Si or Ge; it was also confirmed in our previous work.[5] Furthermore, it was shown[5] that Vegard's law applies well for the $Cd_{1-x}Mn_xGeP_2$ system; i.e., the linearly interpolated lattice constants for $Cd_{1-x}Mn_xGeP_2$ from $CdGeP_2$ (experiment value) and $MnGeP_2$ ("CTB plus $\eta=\eta_{tet}$" value) are very close to available experimental values. Here, we choose the same tetrahedral radii for P, Mn, Zn, Ge, As, and Cd as in Ref. 5, i.e., 1.10, 1.41, 1.31, 1.22, 1.18, and 1.48 Å, respectively. We interpolated $a$ and $c/a$ for $II_{1-x}Mn_xGeV_2$ from the experimental values for $IIGeV_2$ and the "CTB plus $\eta=\eta_{tet}$" value of $MnGeV_2$. All the lattice constants used in the calculations are listed in Table I. The values for $CdGeP_2$ and $CdGeAs_2$ have a larger distortion with respect to the zinc-blende structure, due to the relatively large difference of tetrahedral radii between Cd and Ge. The lattice constant changes due to Mn doping for these Cd systems are smaller than those for the Zn systems because of the closer values of the tetrahedral radii for Cd and Mn. For $Cd_{1-x}Mn_xGeP_2$, the difference with experiment is only 0.4%, as shown in Ref. 5. For $Zn_{1-x}Mn_xGeP_2$, it is reported experimentally that the lattice constants increase with Mn concentration in agreement with Vegard's law.[8] The lattice constants for the sample with $x=0.056$ are measured to be $a=5.479$ Å and $c=10.736$ Å; both are within 0.2% of the values obtained from interpolation for $Zn_{1-x}Mn_xGeP_2$. There are no experimental data available for the crystal structures of $Zn_{1-x}Mn_xGeAs_2$ and $Cd_{1-x}Mn_xGeAs_2$, but the above treatment is expected to give good results.[18]

TABLE I. Lattice constant $a$ (in Å) and $c/a$ used in this work. The experimental lattice parameters for the pure II-Ge-$V_2$ chalcopyrites are taken from Ref. 16 and references therein. Values for $MnGeP_2$ and $MnGeAs_2$ are obtained from "CTB plus $\eta = \eta_{tet}$" rules, and for $x=0.5$ and 0.25, the values of $a$ and $a/c$ are interpolated linearly from $x=0$ and 1.0.

| | $x=0$ | | $x=0.25$ | | $x=0.50$ | | $x=1.00$ | |
|---|---|---|---|---|---|---|---|---|
| | $a$ | $c/a$ | $a$ | $c/a$ | $a$ | $c/a$ | $a$ | $c/a$ |
| $Zn_{1-x}Mn_xGeP_2$ | 5.466 | 1.961 | 5.517 | 1.943 | 5.569 | 1.925 | 5.673 | 1.889 |
| $Zn_{1-x}Mn_xGeAs_2$ | 5.672 | 1.966 | 5.718 | 1.948 | 5.765 | 1.929 | 5.858 | 1.892 |
| $Cd_{1-x}Mn_xGeP_2$ | 5.740 | 1.877 | 5.723 | 1.880 | 5.706 | 1.883 | 5.673 | 1.889 |
| $Cd_{1-x}Mn_xGeAs_2$ | 5.945 | 1.886 | 5.923 | 1.888 | 5.902 | 1.889 | 5.858 | 1.892 |

## IV. ELECTRONIC AND MAGNETIC PROPERTIES: $II_{1-x}Mn_xGeV_2$ SYSTEMS

### A. $MnGeAs_2$ and $MnGeP_2$

$MnGeAs_2$ and $MnGeP_2$ are the simplest cases for these Mn-doped $II_{1-x}Mn_xGeV_2$ systems, and they are suitable for discussing the effects of the anion species. For the AFM configurations, we considered a "spin superlattice" along the [001] direction with alternating magnetic ordering layers. The total energy, Mn-anion bond length and magnetic moments for $MnGeAs_2$ and $MnGeP_2$ obtained from FLAPW calculations are listed in Table II. We find that both the P- and As-based systems are very stable in the AFM alignment. The FM phases are higher in energy by 149 meV/Mn for $MnGeAs_2$ and by 248 meV/Mn for $MnGeP_2$, and their paramagnetic (PM) phases are much higher. The Mn-P and Mn-As bond lengths in the AFM phase are slightly shorter than those in the FM phase, but are much larger than those in the PM phase. The magnetic and electronic properties for both systems are very close, although the energy differences between FM and AFM are quite different in magnitude: the total magnetic moment for the FM state differs by only $0.04\mu_B$ per Mn and the magnetic moments within the Mn muffin-tin spheres also differ by less than $0.06\mu_B$ for both the FM and AFM states. Since Mn substitutes a type-II cation and divalent Mn is expected, a total magnetic moment close to $5.0\mu_B$ per Mn is expected for both systems. However, it is reduced to around $4.3\mu_B$ due to hybridization of the unoccupied Mn spin down $d$ bands with the occupied $p$ bands.

The FM and AFM total densities of states (DOS) of both systems are shown in Fig. 1 and again indicate that the electronic structure has no significant changes for the different anions. Furthermore, we find that there are DOS peaks at the Fermi level in FM $MnGeAs_2$ and $MnGeP_2$, which means that the electronic structure is not stable. In contrast, the AFM phase turns out to be nearly insulator with an energy gap of $\sim 0.58$ eV, which makes the structure stable.

### B. $II_{1-x}Mn_xGeV_2$ for $x=0.25$ and 0.50

The DMol[3] and FLAPW calculated total energy differences between the FM and AFM states of $II_{1-x}Mn_xGeV_2$ (II=Zn or Cd and V=P or As) are listed in Table III for $x=0.25$ and 0.50. For the AFM configurations, we consider "spin superlattices" with alternating magnetically ordered layers along the [100] and [001] directions for $x=0.25$ and $x=0.50$, respectively. The calculated Mn-As and Mn-P bond lengths are almost independent of the magnetic ordering for low Mn composition ($x=0.25$), but are slightly shorter in the AFM state for $x=0.5$, as shown in Table IV.

The AFM state is lower in energy than the FM state for all systems with different Mn compositions, with all energy differences in a small range between $-20$ and $-50$ meV, and is nearly compound independent. The total DOS for FM and AFM $Cd_{1-x}Mn_xGeP_2$ are shown in Fig. 2 as an example; the DOS plots for other systems are very similar. The AFM DOS plot indicates that an energy gap of $\sim 0.28$ eV appears around $E_F$. Unlike the FM DOS for $x=1.0$, the peaks around $E_F$ disappear in the FM DOS plot for $x=0.50$, although there are small tails for both spin-up and spin-down states. Therefore, the FM state electronic structure for $x=0.5$ is more stable than in the $x=1.0$ case, and this is consistent with its total energy being much closer to the corresponding AFM state.

The FLAPW calculated magnetic properties and the Mn-anion bond lengths are listed in Table IV. The total magnetic moments for the FM states are very close to the expected

TABLE II. Comparison of FLAPW calculated relevant structural and magnetic properties of $MnGeP_2$ and $MnGeAs_2$.

| | $MnGeP_2$ | | | $MnGeAs_2$ | | |
|---|---|---|---|---|---|---|
| | FM | AFM | Para | FM | AFM | Para |
| Total energy (meV/Mn) | 0 | −248 | 205 | 0 | −149 | 396 |
| Total magnetic moment ($\mu_B$/Mn) | 4.37 | 0 | – | 4.34 | 0 | – |
| Moment within the Mn MT sphere ($\mu_B$/Mn) | 3.80 | 3.70 | – | 3.84 | 3.76 | – |
| Mn-anion bond length (Å) | 2.44 | 2.43 | 2.31 | 2.52 | 2.51 | 2.38 |

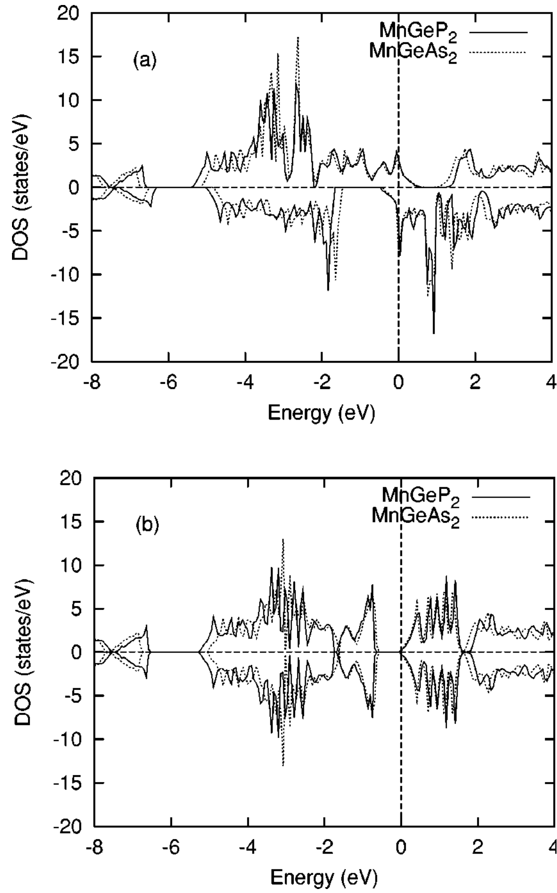


FIG. 1. Total DOS for $MnGeAs_2$ and $MnGeP_2$: (a) FM state and (b) AFM state. The spin-up and spin-down components in this DOS plot, as well as other plots in this paper, are distinguished by positive and negative, repectively.

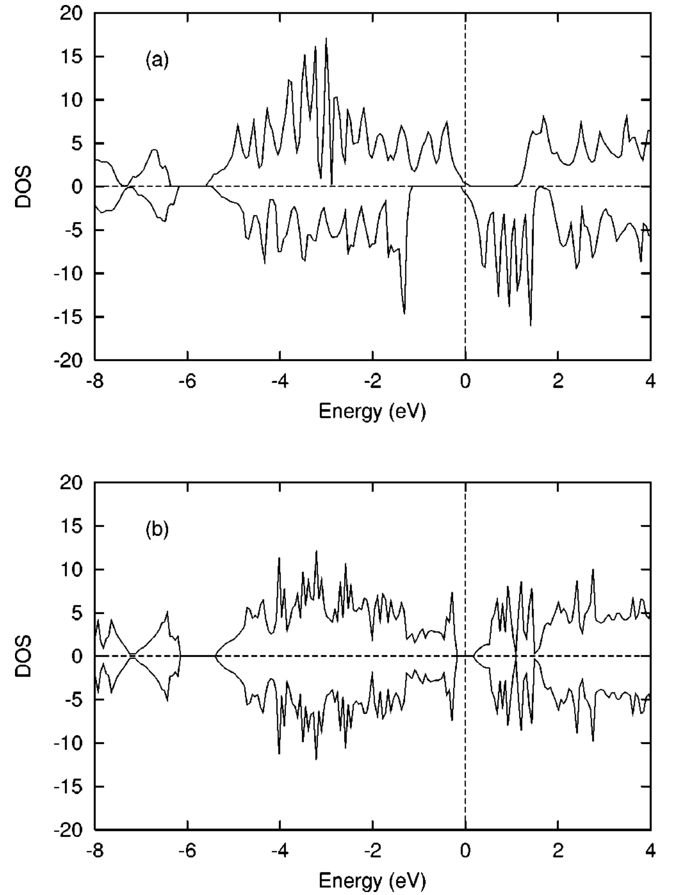


FIG. 2. Total DOS for (a) FM and (b) AFM $Cd_{1-x}Mn_xGeP_2$ at $x=0.50$.

TABLE III. Total energy difference (meV/Mn) between FM and AFM $II_{1-x}Mn_xGeV_2$ for $x=0.25$ and 0.50. The AFM spin superlattice configurations are explained in the text.

| Compound | $Zn_{1-x}Mn_xGeP_2$ | | $Zn_{1-x}Mn_xGeAs_2$ | | $Cd_{1-x}Mn_xGeP_2$ | | $Cd_{1-x}Mn_xGeAs_2$ | |
|---|---|---|---|---|---|---|---|---|
| $x$ | 0.25 | 0.50 | 0.25 | 0.50 | 0.25 | 0.50 | 0.25 | 0.50 |
| $DMol^3$ | −40 | −31 | −32 | −37 | −21 | −35 | −42 | −36 |
| FLAPW | −49 | −26 | −50 | −40 | −30 | −35 | −51 | −35 |

TABLE IV. The FLAPW calculated total magnetic moments, magnetic moment within the Mn MT sphere, and Mn-anion bond length in $II_{1-x}Mn_xGeV_2$ for $x=0.25$ and 0.5.

| | | Bond length (Å) | | Total moment ($\mu_B$/Mn) | | Mn moment ($\mu_B$) | |
|---|---|---|---|---|---|---|---|
| Compound | $x$ | FM | AFM | FM | AFM | FM | AFM |
| $Zn_{1-x}Mn_xGeP_2$ | 0.25 | 2.39 | 2.39 | 5.00 | 0 | 3.83 | 3.76 |
| | 0.50 | 2.41 | 2.40 | 4.99 | 0 | 3.89 | 3.84 |
| $Zn_{1-x}Mn_xGeAs_2$ | 0.25 | 2.46 | 2.46 | 5.00 | 0 | 3.98 | 3.90 |
| | 0.50 | 2.48 | 2.47 | 4.96 | 0 | 3.91 | 3.84 |
| $Cd_{1-x}Mn_xGeP_2$ | 0.25 | 2.43 | 2.43 | 5.00 | 0 | 3.91 | 3.86 |
| | 0.50 | 2.44 | 2.43 | 5.00 | 0 | 3.92 | 3.88 |
| $Cd_{1-x}Mn_xGeAs_2$ | 0.25 | 2.50 | 2.50 | 5.00 | 0 | 3.93 | 3.88 |
| | 0.50 | 2.50 | 2.49 | 4.97 | 0 | 3.94 | 3.88 |

TABLE V. The DMol[3] calculated formation energy, $E^f$ (eV), for Si and S substituting the P or Ge sites in $Cd_{1-x}Mn_xGeP_2$ at $x=0.25$. P1 represents the P sites close to Mn, and P2 represents other P sites. In the calculations, the internal structures are fully optimized, while the lattice volume is assumed to be the same as that without S or Si impurities.

| Impurity | P1 | P2 | Ge |
|---|---|---|---|
| Si | 1.37 | 1.47 | −0.52 |
| S | 0.14 | 0.16 | 1.80 |

value of $5.0\mu_B$ per Mn since the Mn $3d$ spin-down states are nearly unoccupied. The total FM magnetic moments of As systems for $x=0.5$ have a little bit smaller value than those of P. That is, more Mn $3d$ (which are mixed with anion $p$ states) spin-down states are occupied in the As systems because As $4p$ states are more delocalized in energy than are the P $3p$ states. The magnetic moments within Mn muffin-tin spheres are close to $4.0\mu_B$ in the FM states, but are only $0.04\mu_B$–$0.08\mu_B$ smaller in the corresponding AFM states. This suggests that the spin moments are very localized at the Mn site. The small energy difference between FM and AFM also suggests that the spin moments are weakly coupled.

To sum up, all the systems are energetically stable in the AFM phase at $T=0$ K, and the various electronic and magnetic properties are very similar to each other. The lattice size effect for magnetic properties does not appear as expected in the Mn-doped III-V systems,[19] since there are no holelike carriers showing up.

### V. FM STABILIZATION OF $Cd_{1-x}Mn_xGeP_2$ BY S

As discussed above, the $II_{1-x}Mn_xGeV_2$ systems are all AFM favored; however, there may still be possible ways to obtain a FM ground state. For example, according to Ferrand *et al.*,[20] an AFM to FM transition was found in $Zn_{1-x}Mn_xTe$ epitaxial layers due to holes induced by nitrogen doping. Here, we investigate the possible transition induced by impurities in $II_{1-x}Mn_xGeV_2$ systems, exemplified by $Cd_{1-x}Mn_xGeP_2$. To begin with, Si and S are easily seen to be good choices for impurity-induced carriers, since they are same row neighbors of P in the Periodic Table. First, we calculated the formation energy for Si or S substituting P or Ge sites with the DMol[3] method with a unit cell of $Cd_3MnGe_4P_8$, i.e., $x=0.25$. The formation energy defined as the total energy difference between reactants and products is calculated for S substituting P as

$$E^f=E_{tot}(Cd_3MnGe_4P_7S)+E_{tot}(P)-E_{tot}(Cd_3MnGe_4P_8)-E_{tot}(S), \tag{5}$$

where $E_{tot}$ represents the total energy of the system.[21] The formation energies for other substitutions calculated similarly are listed in Table V. It is found that while Si easily goes into the Ge site rather than the P site because their valences match, this will not be helpful in producing carriers. On the other hand, S prefers P sites rather than Ge sites with $E^f$ around 0.14 eV. We assume that the S could be doped in the $Cd_{1-x}Mn_xGeP_2$ system at certain concentrations and study the effect of its doping on the magnetic properties of $Cd_{1-x}Mn_xGeP_2$.

TABLE VI. The FLAPW and DMol[3] calculated energy difference between FM and AFM $Cd_{1-x}Mn_xGeP_{1.75}S_{0.25}$ for $x=0.25$, 0.5, and 1.0. The internal structures are optimized by DMol[3].

| | $\Delta E=E_{AFM}-E_{FM}$ (meV/Mn) | |
|---|---|---|
| $x$ | DMol[3] | FLAPW |
| 0.25 | 44.6 | 51.7 |
| 0.50 | 11.1 | 26.9 |
| 1.00 | −176.6 | −175.5 |

With 12.5% P substituted by S, the internal structures of FM and AFM $Cd_{1-x}Mn_xGeP_2$ are optimized by DMol[3] with the AFM configurations set in the same "spin superlattice" as before. As calculated by both the FLAPW and DMol[3] methods, the total energy differences between FM and AFM states for $x=0.25$, 0.5, and 1.0 are listed in Table VI. For $x=1.0$, $Cd_{1-x}Mn_xGeP_2$ still keeps AFM as its stable phase, but the energy difference from the FM phase is reduced by ~72 meV/Mn when S is introduced. For $x=0.25$ and 0.50, the total energy of the FM state becomes lower than that of the AFM state; i.e., an AFM to FM phase transition is found due to S doping.

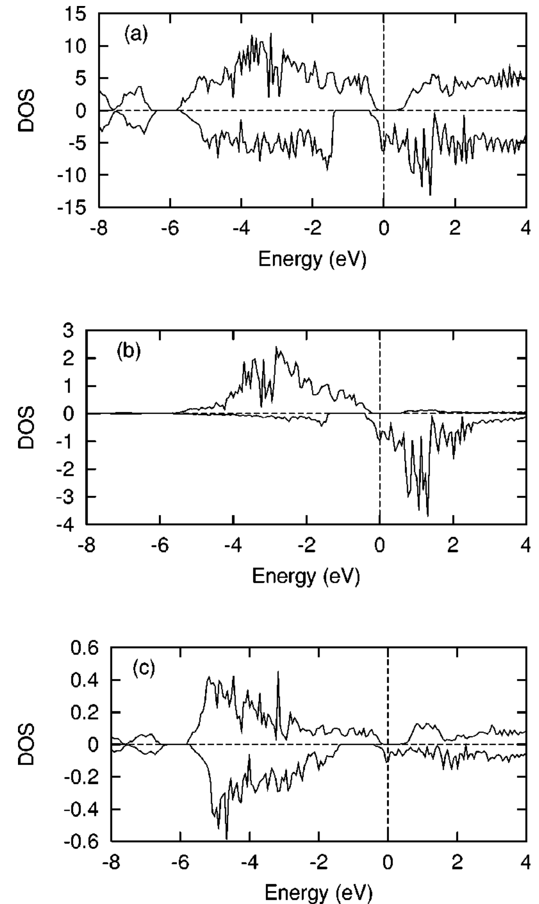


FIG. 3. (a) Total DOS, (b) Mn $3d$, and (c) S $3p$ projected DOS for FM $Cd_{1-x}Mn_xGeP_{1.75}S_{0.25}$ for $x=0.50$.

To examine the effect of S doping on its electronic structures, the total DOS and projected Mn $3d$ and S $3p$ DOS for $x=0.50$ are shown in Fig. 3. Obviously, the Fermi level is shifted to higher energy [cf. Fig. 2(a) and Fig. 3(a)] due to the additional electron introduced by S substituting P. The total DOS indicates that the additional electron fills in the spin-down bands and makes the system half-metallic. Therefore, each doped S will reduce the magnetic moment of the system by $1\mu_B$: the calculated total magnetic moments come out to be $4.5\mu_B$ per Mn for $x=0.50$ and $4.0\mu_B$ per Mn for $x=0.25$, respectively, due to the corresponding Mn:S ratio (2:1 for $x=0.50$ and 1:1 for $x=0.25$). In order to see the effect of S concentration, we also studied $Cd_{1-x}Mn_xGeP_2$ for $x=0.25$ with P substituted by 6.25% S. The $DMol^3$ calculated energy difference between FM and AFM is 40.0 meV/Mn, i.e., very close to that of the 12.5% S case. This confirms that the AFM to FM phase transition will also occur at lower S concentration. The total magnetic moment for $Cd_{0.75}Mn_{0.25}GeP_{1.875}S_{0.125}$ is $4.5\mu_B$/Mn, in excellent agreement with the above discussion on the Mn:S ratio.

As a result, the total magnetic moments may be tuned easily by the impurity concentrations, which will be a great boon for technological applications. The projected DOS shows that the Mn $3d$ spin-up bands are fully occupied and the spin-down bands are partially filled due to the shift of $E_F$; the S $3p$ bands are also strongly spin split due to the hybridization with Mn $3d$ bands. The fact of an induced magnetic order transition once again shows the important role of carriers in FM semiconductors. The room-temperature ferromagnetism in $Zn_{1-x}Mn_xGeP_2$ (without carriers) and the FM to AFM phase transition below 47 K are novel phenomena and their origin is still unclear. Obviously, more theoretical and experimental studies are called for.

## ACKNOWLEDGMENTS

This work was supported by the NSF (through the Materials Research Center at Northwestern University) and a grant of computer time at the San Diego Supercomputing Center.

---

*Present address: Fritz-Haber-Institut der Max-Planck-Gesellschaft, Faradayweg 4-6, D-14195 Berlin, Germany.

[1] H. Ohno, Science **281**, 951 (1998); Y. Ohno, D.K. Young, B. Beschoten, F. Matsukura, H. Ohno, and D.D. Awschalom, Nature (London) **402**, 790 (1999).

[2] H. Ohno, J. Magn. Magn. Mater. **200**, 110 (1999).

[3] *Diluted Magnetic Semiconductors, Semiconductors and Semimetals*, edited by J. K. Furdyna and J. Kossut (Academic Press, Boston, 1986), Vol. 25.

[4] G.A. Medvedkin, T. Ishibashi, T. Nishi, K. Hayata, Y. Hasegawa, and K. Sato, Jpn. J. Appl. Phys., Part 2 **39**, L949 (2000).

[5] Yu-Jun Zhao, W.T. Geng, A.J. Freeman, and T. Oguchi, Phys. Rev. B **63**, R201202 (2001).

[6] E. Wimmer, H. Krakauer, M. Weinert, and A.J. Freeman, Phys. Rev. B **24**, 864 (1981), and references therein.

[7] B. Delley, J. Chem. Phys. **113**, 7756 (2000).

[8] S. Cho *et al.* (unpublished).

[9] B. Delley, J. Chem. Phys. **92**, 508 (1990).

[10] W.T. Geng, Yu-Jun Zhao, A.J. Freeman, and B. Delley, Phys. Rev. B, **63**, 060101 (2001).

[11] B. Delley, Int. J. Quantum Chem. **69**, 423 (1998).

[12] J.P. Perdew, K. Burke, and M. Ernzerhof, Phys. Rev. Lett. **77**, 3865 (1996).

[13] Yu-Jun Zhao, W.T. Geng, K.T. Park, and A.J. Freeman, Phys. Rev. B **64**, 035207 (2001).

[14] Yu-Jun Zhao, W. T. Geng, A. J. Freeman, and B. Delley, Phys. Rev. B (to be published).

[15] A. Continenza, S. Picozzi, W.T. Geng, and A.J. Freeman, Phys. Rev. B **64**, 085204 (2001).

[16] J.E. Jaffe and A. Zunger, Phys. Rev. B **29**, 1882 (1984).

[17] S.C. Abrahams and J.L. Bernstein, J. Chem. Phys. **59**, 5415 (1973).

[18] As an extensive test, we found that the $DMol^3$ calculated energy difference between FM and AFM changes by only 3 meV when $a$ and/or $c$ is enlarged, or reduced, by 1%. This indicates that the *energy difference* is not strongly sensitive to the lattice constant $a$ and $c$.

[19] T. Dietl, H. Ohno, J. Cibert, and D. Ferrand, Science **287**, 1019 (2000).

[20] D. Ferrand *et al.*, Phys. Rev. B **63**, 085201 (2001).

[21] The total energies for Si and Ge are taken from their bulk crystal values. The bulk P and S crystal structures are very complicated, but they are packed with $P_4$ [A. Simon *et al.*, Phosphorus, Sulfur Silicon Relat. Elem. **30**, 507 (1987)], and $S_8$ [G.S. Pawley and R.P. Rinaldi, Acta Crystallogr., Sect. B: Struct. Crystallogr. Cryst. Chem. **28**, 3605 (1972)] molecular units. Since the interaction between the molecules is very weak, the total energies of P and S are taken from calculations on $P_4$ and $S_8$ clusters, respectively, using the molecular version of $DMol^3$.